Physical models to evaluate the performance of impure phase change material dispersed in building materials

Y. Khattari, H. El-Otmany, T. El Rhafiki, Tarik Kousksou, A. Ahmed, E. Ben Ghoulam

Physical models to evaluate the performance of impure phase change material dispersed in building materials

Y. Khattari[(a)], H. El-Otmany[(b)], T. El Rhafiki[(c)] , T. Kousksou[(d)] , A. Ahmed[(a)] , E. Ben Ghoulam[(a)]

[(a)]Department of Physics, Faculty of Sciences, Moulay-Ismaïl University, Meknes, Morocco
[(b)]Laboratory of Mathematics and its Application of Pau, IPRA, UMR5142,
E2S-University of Pau, 64000 Pau, France
[(c)]Engineering Sciences Laboratory, Polydisciplinary Faculty of Taza, Sidi Mohamed Ben Abdellah University Fez Morocco
[(d)]Universite de Pau et des Pays de l'Adour, E2S UPPA, SIAME, Pau, France

Abstract

Currently, the introduction of phase change materials (PCM) in building materials is recognized as a popular technique for reducing interior temperature fluctuations and improving the energy efficiency of buildings. Conventionally, PCM in construction materials is different with bulk PCM as it incorporates impurities and acts as a binary mixture. For this reason, physical models to describe heat transfers inside such materials are highly requested. This paper presents four physical approaches that can be applied to examine heat transfer in impure PCM dispersed inside a building material. These models have been successfully verified and tested using experimental results from the literature. A significant hysteresis is observed during the phase transition as a result of thermal gradients within the composite material as well as the non-symmetric enthalpy profile as a function of temperature.

Keywords: PCM ; Physical models ; Building material ; Latent storage; Hysteresis.

1- Introduction

The building sector in Europe is one of the most energy consuming areas in the world due to its heating and cooling systems. As reported by the International Energy Agency (IEA), the sector produces about 1/3 of total greenhouse gas emissions **[1-2]**. It is therefore crucial to develop new approaches for saving energy and limiting energy use, without restricting the development of the building sector [**3-4**]. In this context, an appropriate design of the building enclosure has a decisive role to ensure a reduction in the building's energy use and to preserve the thermal comfort of the residents [**5-6**]. Several passive strategies to improve the building's energy performance have recently been implemented [**7-8**]. As a complement to these strategies, the integration of phase change materials (PCM) in construction materials is recently recognized as a popular technique for reducing interior temperature fluctuations and improving the energy efficiency of buildings [**9-10**]. In building, the PCM not only was used in the surrounding envelopes **[11],** but also in the ceiling **[12],** floor **[13]**, and energy equipment **[14-15].** When the PCM is used in the buildings, the thermal stability should also be tested first. Some researchers have carried out nearly 4,000 cooling-heating thermal cycles to experimentally investigate it **[16-17].** For this reason, physical models to describe heat transfers inside such materials are highly requested. However, the implementation and verification of such models is a challenging exercise due to the non-linearity of the solid-liquid phase change [**18**].

Realistic simulation of heat transfer in a composite material incorporating PCM is an important challenge. However, due to the non-linearity of heat transfer during the solid-liquid phase change **[19]**, a restricted number of analytical solutions are available, while numerical solutions are largely accessible. They can be consulted in the leading papers on heat transfer, such as Crank **[20]**, Hill **[21],** Voller **[22]** and Alexiades and Solomon **[23].** Additionally, it should be noted that the analytical solution for an ideal isothermal phase transition case may not be able to produce a complete representation of the composite material containing PCM. Generally, PCMs used in the construction materials of the building are impure and act like binary mixtures **[24-25],** which mean that the phase change processes in these materials are not isothermal and often carried out within a range of temperature **[26-27].** Other technical aspects like hysteresis phenomenon can also complicate the modelling of phase transition in building materials **[28-29].** This phenomenon is typically marked by a total displacement of

the enthalpy function during the freezing process of the PCM compared to the same one along the fusion process **[30-31].** In this context, some of the analytical and numerical solutions described earlier may give some useful insights, but may be not suitable for composite materials including PCMs **[32-33].**

A number of numerical methods are available in the literature for modeling PCMs, particularly the apparent heat capacity method (AHCM) [**34-35**], the heat source method (HSM) [3**6-37**], the explicit enthalpy method (EEM) [**32**] and the implicit enthalpy method (IEM) [**38-39]**. However, the number of studies published in the literature that compare the results of these models with experimental ones and that outline the advantages and disadvantages of each approach is limited [**40-41**]. It is interesting to mention that there are few experimental studies that provide all the necessary information to validate physical models describing heat transfers in a composite PCM **[32, 42].** This includes both the accurate description of all the boundary conditions applied to the physical domain during the charging/discharging period, and precise determination of various thermophysical properties of the PCM-based materials adopted for the experiments.

A precise determination of the heat capacity and enthalpy functions of impure materials during the phase transition process is also essential for a correct mathematical modelling of heat transfer within the composite material. Whatever the physical model, if such functions are employed, they may be a potential source of imprecision **[43].** Usually, specific enthalpy and specific heat capacity of a PCM versus temperature are commonly determined using the DSC device. However, the precision of this apparatus relies on the accuracy of the protocol employed to describe the phase change characteristic of the PCM. When performing DSC experiments, particular consideration must be paid to the choice of the scan rates, as various heating rates provide various outputs for heat flux and phase transition temperatures**.** In this work, the apparent heat capacity function of an impure PCM is determined from an enthalpy function, which is deduced from an inverse method presented in detail in Ref. **[44].**

To our best knowledge, a few numerical models are reported in the literature addressing the phase change process of impure PCMs dispersed in building material [32]. In this paper, four physical models are implemented to characterize heat transfers in a building component with an impure PCM. It particularly examines the feasibility of these methods for building applications. The experimental works of Joulin et al. [**42**] and Franquet et al. [**32**] were

selected to verify these physical models. The merits and drawbacks of each physical model will be outlined and commented in the following sections of this work.

2. Fluxmeter Device

It is important to outline that phase transition characterization is a key point concerning both the thermal performance and the conception of composite PCMs. Storage density and melting temperatures are among the main design criteria of the composite material containing impure PCM. In addition, reliable mathematical models that accurately describe the heat transfer inside a composite PCM require accurate information on the heat capacity and enthalpy functions of these materials during the phase transition process.

Regardless of the physical model, if such functions are used, they could represent a possible source of inaccuracy **[32, 45].** A number of researchers use the DSC device to measure the specific enthalpy and the heat capacity of the PCM as a function of temperature [**46**]. However, the DSC's accuracy depend on the precision of the protocol adopted to describe the phase transition. The selection of the scan rate should be done carefully during the DSC experiments, since different heating rates can afford different outputs for heat flux and phase transition temperatures **[47-48].** This problem can be solved using a simplest and inexpensive technique to determine both latent heat and the melting point of PCMs namely T-history technique **[49-50].** Using this method, the material size is significantly larger and the effect of the non-homogeneity of the sample can be considered when carrying out the thermal characterization of the building material. However, despite the advantages of the T-history technique, it is not suitable to use this method to determine the enthalpy of large-scale of composite PCM **[51**]. The fluxmeter is commonly employed by several researchers to thermally characterize composite materials incorporating PCM **[45].** The main advantage of this device is the ability of testing building material samples in cement blocks or in panel form, which helps to avoid the problems caused by the small mass of the sample [**52**]. Furthermore, several studies are already used this apparatus in order to validate the physical models that describe the thermal behaviour of composites PCM **[32, 42].**

The fluxmeter device is currently one of the instruments that used extensively to determine the thermophysical properties of composite PCM **[46, 53]**. It is interesting to note that this

device (see **Fig.1**) is unable to provide insight regarding the thermal gradients in the composite material during the phase transition process. The fluxmeter provides only temperature (T_p) and heat flux ($\emptyset$) measurements at the material extremities. In this paper, the numerical models presented in section 3 are used to determine the temperature variations inside the composite PCM. In addition, these models are verified and validated using the experimental heat fluxes provided by the fluxmeter device **[32].** In Ref. **[32]**, the mortar including 12.5% of microencapsulated PCM is disposed in a parallelepipedic form with dimension of 25×25×4 cm^3 [**32**]. A rectangular composite material containing microencapsulated PCM is used as a sample in this study, and each face of it is subjected to a linear plate temperature T_p (**see Eq.1**) which is dependent on time and ranging from 7 to 39°C over time by using different heating/cooling rates β.

$$T_p = \beta t + T_o \quad \textbf{(1)}$$

where β is the heating/cooling rate and T_o the temperature of the composite material at $t = 0$.

Table 1 showed the thermophysical properties of the composite material **[32].**

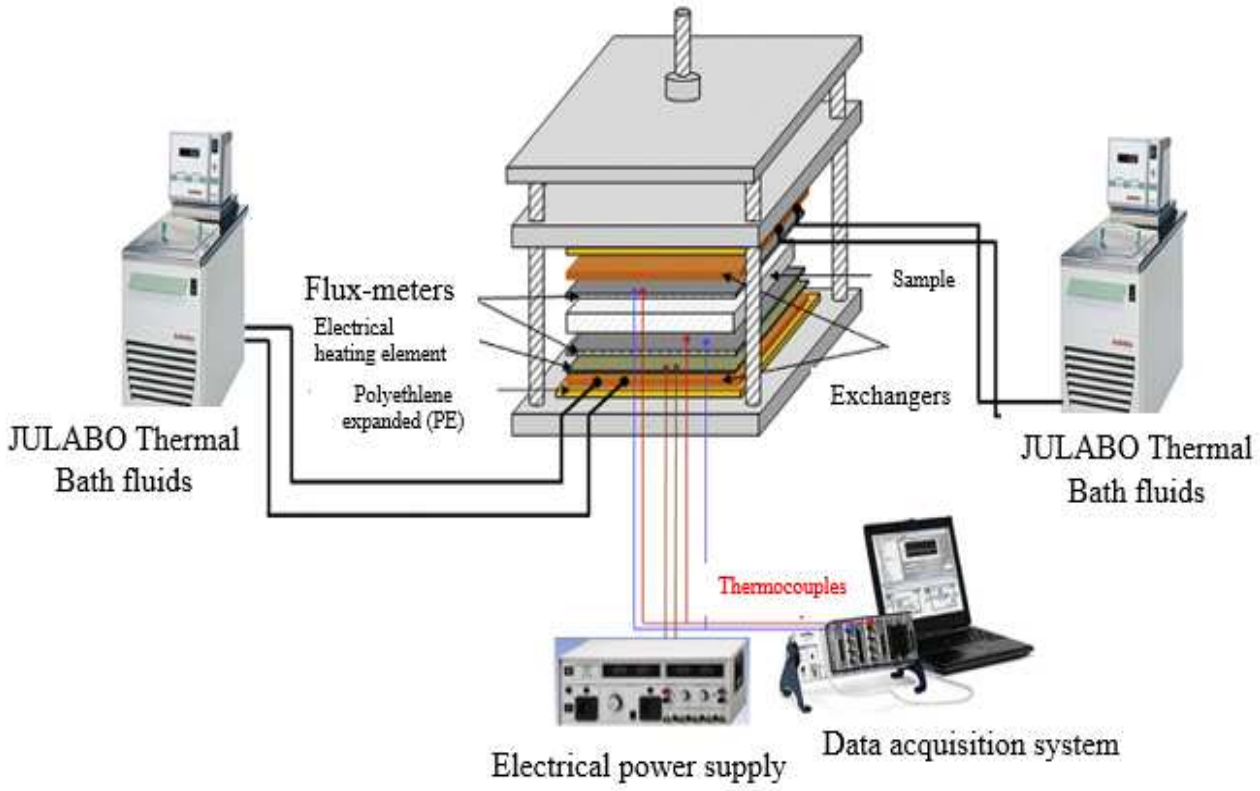

Fig.1: Fluxmeter device **[32]**

Table 1: Thermophysical properties of composite phase change material

ρ	1412 kg.m^{-3}
k	0.55 W.m^{-1}.°C^{-1}
c_S	1100 J.kg^{-1}°C^{-1}
c_L	1070 J.kg^{-1}°C^{-1}
L_f	12 J.g^{-1}
T_m	25.5 °C
T_A	26.8 °C

3. Mathematical models

The physical models that we will present in the succeeding paragraphs are based on the following hypotheses:

- The composite material consists of two elements: mortar and PCM.
- The PCM is impure and acts as a binary mixture.
- The thermal conduction is unidirectional in the x-axis.

3.1 Apparent heat capacity method (AHCM)

When the physical model is derived from the apparent calorific capacity approach, the heat transfer inside the composite PCM can be described by a single energy equation **[54],** i. e.

$$\rho_c c_{app}(T)\frac{\partial T(x,t)}{\partial t} = k_c \frac{\partial^2 T(x,t)}{\partial x^2} \quad \textbf{(2)}$$

where ρ_c and k_c are the density [kg/m^3] and the thermal conductivity [W/(m.K] of the composite material including PCM respectively. *T* and *t* represent temperature (°C) and time (s) and $c_{app}(T)$ denotes the apparent heat capacity [kJ/(kg.K)].

The $c_{app}(T)$ function in **Eq. 2** can be defined as **[55]** :

$$c_{app}(T) = \frac{dh(T)}{dT} \tag{3}$$

where h is the enthalpy of the construction material and may be obtained by considering the formula below:

$$h(T) = \varepsilon.h_{pcm} + (1-\varepsilon).h_{mortar} \tag{4}$$

where ε is the mass fraction of the PCM in the composite material.

Eq. (3) can be expressed as :

$$c_{app}(T) = \varepsilon.\frac{dh_{pcm}}{dT} + (1-\varepsilon).\frac{dh_{mortar}}{dT} = \varepsilon.c_{pcm}(T) + (1-\varepsilon).c_{mortar} \tag{5}$$

In **Eq.(5),** the mortar enthalpy is an usual sensible enthalpy, while the enthalpy of the PCM should be defined during both sensible and latent storage.

It can be noted that according to equations (2) and (5), the physical model can provide a clear description of the phase transition inside the composite material as long as the specific thermal capacity of the PCM is adequately defined.

In this work, the correlation developed by Franquet et al. **[32]** is selected to determine the value of the apparent heat capacity of PCM behaving as a binary mixture:

$$c_{pcm}(T) = \begin{cases} c_{s,pcm} + \left(c_{L,pcm} - c_{S,pcm}\right) \times \left(\frac{T_A - T_m}{T_A - T}\right) + L_f \times \frac{T_A - T_m}{\left(T_A - T\right)^2} & if \quad T \prec T_m \\ c_{L,pcm} & if \quad T \geq T_m \end{cases} \tag{6}$$

where T_m represents the end of the non-isothermal melting of the PCM,T_A is the melting temperature of the pure PCM and L_f is the latent heat of fusion. The first two terms in **Eq.6** reflect the sensible part and the last one describes the variation of the latent fusion throughout the phase transition of the PCM.

By using **Eq.(6),** one can analyze and explain the non-isothermal phase change in PCMs behaving as a binary solutions**.** By fixing the reference point $h(T_A)=0$**,** an analogous expression can be deduced for the specific enthalpy of the composite material containing microencapsulated PCM **[32]**:

$$h\,(T)=\begin{cases} c_S\left(T-T_m\right)+c_L\left(T_m-T_A\right)-\varepsilon L_f\left(1-\dfrac{T_A-T_m}{T_A-T}\right)+\left(c_S-c_L\right)\left(T_A-T_m\right)\ln\left(\dfrac{T_A-T}{T_A-T_m}\right) & if \quad T\prec T_m \\ c_L\left(T-T_A\right) & if \quad T\geq T_m \end{cases} \qquad \textbf{(7)}$$

where $c_i=\varepsilon.c_{i,pcm}(T)+\left(1-\varepsilon\right).c_{mortar}$ (i being either Solid or Liquid).

Fig.2 illustrates the variation of the specific enthalpy versus temperature for two cases: $T_m < T_A$ and $T_m = T_A$. During the heating process, the state of the composite material displaces from left to right across the curve, with increasing enthalpy and temperature. In a first step, the temperature of the PCM increases with the additional energy that is stored as sensible heat in the solid PCM. The latent heat of fusion is absorbed as the PCM passes from solid phase to liquid phase. When the melting process is concluded, additional energy input again results in a temperature increase (sensible heat in liquid phase). We note that in the case of $T_m < T_A$, the PCM behaves like a binary mixture and the melting process is carried out over a range of temperatures. However, in the case of $T_m = T_A$ the PCM acts as a pure substance and the phase transition process is done at constant temperature.

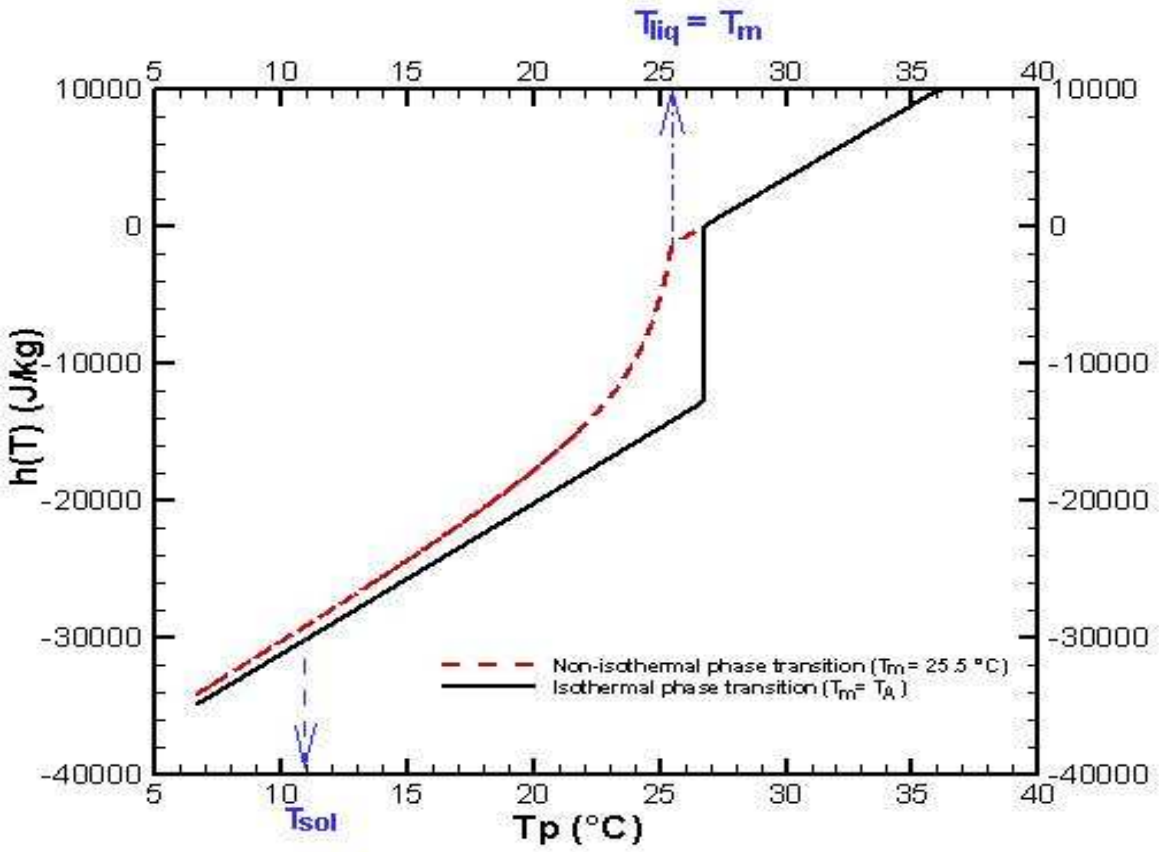

Fig.2: Specific enthalpy versus temperature

The energy equations **(2)** were discretized over each control volume by using the finite volume approach **[55]**. A fully implicit scheme was implemented in time. The uniform size of the control volumes and constant time steps have been applied. The resultant finite volume equations are represented by the following formulas:

$$a_i T_i^{n+1} = a_{i+1} T_{i+1}^{n+1} + a_{i-1} T_{i-1}^{n+1} + b_i \qquad \textbf{(8)}$$

where:

$$a_{i+1} = a_{i-1} = \frac{k_c}{\Delta x} \qquad \textbf{(9)}$$

$$a_i = a_{i-1} + a_{i+1} + \frac{\rho_c \, c_{app}(T_i^n)}{\Delta t} \qquad \textbf{(10)}$$

$$b_i = \frac{\rho_c \, c_{app}(T_i^n)}{\Delta t} \times T_i^n \qquad \textbf{(11)}$$

As shown in **Eqs (10)** and **(11)**, the apparent heat capacity of the composite material is calculated at the previous time (n) by using **Eq.6.**

In this paper, **Eqs.(8)** were solved iteratively by using a Tridiagonal Matrix Algorithm (TDMA) method **[55]**. The computation procedure was carried out using Fortan. The specified iteration in each time interval was considered convergent when the maximum relative residual of T was less than 10^{-4}.

3.2 Enthalpy method

The so-called enthalpy approach has been established to address phase change problems for such applications **[22].** Therefore, the enthalpy method can be adopted for the solution of phase change problems inducing both isothermal phase transition (i.e. the phase change taking place at a constant temperature) as well as non-isothermal phase transition (i.e. the phase change taking place over a range of temperatures) (see **Fig.2**). We will now describe the application of the enthalpy method for the solution of one-dimensional fusion or solidification inside the composite phase change material using both explicit and implicit finite volume schemes.

For conduction-driven heat transfer, the energy equation can be rewritten into one equation where latent heat is integrated into the enthalpy term as shown below :

$$\rho_c \frac{\partial h(x,t)}{\partial t} = k_c \frac{\partial^2 T(x,t)}{\partial x^2} \qquad \textbf{(12)}$$

which is assumed to be applicable to the overall solution domain, comprising the solid phase and the liquid phase as well as the solid-liquid interface. **Eq. 12** can be resolved by two different techniques: the explicit enthalpic method or the implicit enthalpic method.

3.2.1 Explicit enthalpy method (EEM)

The finite volume approximation of **Eq.(12)** with simple explicit enthalpy method is obtained as **[32]**:

$$h_i^{n+1} = h_i^n + a_{i-1}T_{i-1}^n + a_i T_i^n + a_{i+1}T_{i+1}^n$$

(13)

where :

$$a_{i+1} = a_{i-1} = \frac{k_c}{\rho_c}\frac{\Delta t}{(\Delta x)^2}$$

(14)

$$a_i = -2\frac{k_c}{\rho_c}\frac{\Delta t}{(\Delta x)^2}$$

(15)

As the **Eq.13** is explicit, the following condition should be satisfied for stability:

$$\frac{k_c}{\rho_c c_c}\frac{\Delta t}{(\Delta x)^2} \prec \frac{1}{2}$$

(16)

The following algorithm can be used to solve explicit finite volume element equations for the enthalpy method.

We assume that the numerical solution has progressed as far as the time level and the numerical values of T_i^n and h_i^n are known. The relationship between enthalpy function and temperature can be derived from experimental data or standard physical tables. Generally, enthalpy is a non-linear function of temperature. The enthalpies and temperatures at the next time level can be determined as follows :

(i) Compute h_i^{n+1} from **Eq. 13**.

(ii) Compute the corresponding T_i^{n+1} from **Eq.7** by using the value of h_i^{n+1} :

$$T_i^{n+1} = \begin{cases} F^{-1}(h_i^{n+1}) & if \quad h_i^{n+1} \prec h_m \\ \dfrac{h_i^{n+1}}{c_L} + T_A & if \quad h_i^{n+1} \geq h_m \end{cases}$$

(17)

where $F^{-1}(h_i^{n+1})$ is the inverse function of h_i^{n+1}.

To avoid the calculation of the inverse function of h_i^{n+1}, it is possible to approximate the enthalpy curve $h(T)$ during the melting process by a smooth curve between two neighbouring points.

3.2.2 Implicit enthalpy method (IEM)

The finite volume approximation of **Eq.(12)** with simple implicit enthalpy method is obtained as [41]:

$$h_i^{n+1} = h_i^n + a_{i-1}T_{i-1}^{n+1} + a_i T_i^{n+1} + a_{i+1}T_{i+1}^{n+1}$$

(18)

According to Eq.(18), it is clear that the new value of the enthalpy function h_i^{n+1} at node *i* is dependent on the new value of temperatures T_{i-1}^{n+1}, T_i^{n+1} and T_{i+1}^{n+1} and therefore the enthalpy function is nonlinear. **Eq.(18)** cannot be solved without using proper numerical techniques to handle this nonlinearity. A practical way to overcome this nonlinearity is to approximate the enthalpy curve (see Eq.(7)) during the phase change transition process by a piecewise linear function. For example, we could use a linear approximation to describe the enthalpy curve during the melting process:

$$h_i^{n+1} = b_{i,1}T_i^{n+1} + b_{i,2}$$

(19)

Where $b_{i,1}$ and $b_{i,2}$ are the constant coefficients.

Using **Eq.(19)**, **Eq.(18)** can be written as follows:

$$a_{i-1}T_{i-1}^{n+1} + a_i^{'}T_i^{n+1} + a_{i+1}T_{i+1}^{n+1} = h_i^{n'}$$

(20)

where:

$a_i^{'} = a_i - b_{i,1}$ and $h_i^{n'} = b_{i,2} - h_i^n$

Eq.(18) becomes linear equation (see **Eq.(20)**) with one primary dependent variable « Temperature » that can be iteratively solved using a Tridiagonal Matrix Algorithm (TDMA) method [55]. The TDMA algorithm is faster because there are no restriction on the time step.

3.3 Heat source method (HSM)

The energy equation using the heat source approach can be expressed as follow [39-40]:

$$\rho_c c_c \frac{\partial T(x,t)}{\partial t} = k_c \frac{\partial^2 T(x,t)}{\partial x^2} - \rho_{pcm} L_f \frac{\partial f}{\partial t} \quad \textbf{(21)}$$

Where f is the liquid fraction of the PCM.

The finite volume discretization of **Eq.(21),** based on a fully implicit time integration has the following expression:

$$a_i T_i^{n+1} = a_{i+1} T_{i+1}^{n+1} + a_{i-1} T_{i-1}^{n+1} + b_i$$

(22)

where:

$$a_{i+1} = a_{i-1} = \frac{k_c}{\Delta x}$$

(23)

$$a_i = a_{i-1} + a_{i+1} + \frac{\rho_c c_c}{\Delta t} \Delta x$$

(24)

$$b_i = \frac{\rho_c c_c}{\Delta t} \Delta x \times T_i^n - \rho_{pcm} L_f \frac{f_i^{n+1} - f_i^n}{\Delta t} \Delta x$$

(25)

For the isothermal phase change (i.e. $T_m = T_A$ (see **Fig.2**)), the liquid fraction can estimated at each time step, using the method reported in **[22]**:

$$f_i^{n+1} = f_i^n + \frac{a_i T_i^n}{\rho_{pcm} L_f \frac{\Delta x}{\Delta t}}$$

(26)

The liquid fraction is updated at each node using the following corrections:

$$f = \begin{cases} 0 & if\ f \le 0 \\ 1 & if\ f \ge 1 \end{cases}$$

(27)

For the phase change over a range of temperature from T_{sol} to T_{liq}, the liquid fraction can be estimated using the following expression:

$$f_i^{n+1} = \frac{T_i^{n+1} - T_{sol}}{T_{liq} - T_{sol}} \quad \textbf{(28)}$$

In **Eq.28**, the enthalpy function can be approximated by a piecewise linear function (see **Eq.19)**. Using **Eq.(19)** and **Eq.(28), Eq.(22)** can be written as follows:

$$a_i^{'}T_i^{n+1} = a_{i+1}T_{i+1}^{n+1} + a_{i-1}T_{i-1}^{n+1} + b_i^{'} \quad \textbf{(29)}$$

Where : $a_i^{'} = a_i + \frac{\rho_{pcm} L_f b_{i,1} \Delta x}{\left(h_{liq} - h_{sol}\right)\Delta t}$ and $b_i^{'} = (\rho_c c_c + \frac{\rho_{pcm} L_f b_{i,1}}{\left(h_{liq} - h_{sol}\right)})\frac{\Delta x}{\Delta t} T_i^n$

The liquid fraction is updated at each node using the following corrections:

$$f = \begin{cases} 0 & if\ T \prec T_{sol} \\ 1 & if\ T > T_{liq} \end{cases}$$

(30)

For both isothermal and non-isothermal phase change, **Eqs. 22 and 29** can be solved iteratively using the TDMA algorithm.

It is important to mention that for the three physical models (AHCM, IEM and HSM), the space grid size of the composite PCM is 0.2 mm and the time step is 1 min. Further refinement of either space grids or time steps has no impact on the numerical results. The specified iteration in each time interval was considered convergent when the maximum relative residual of T was less than 10^{-4}.

The main advantage of the EEM is its simplicity of programming. The drawback of the EEM is that the temperature of a grid point can only be calculated at specific times. In addition, as **Eq.13** is explicit, the following condition should be satisfied for stability:

$$\frac{k_c}{\rho_c c_c}\frac{\Delta t}{(\Delta x)^2} \prec \frac{1}{2}$$

(31)

In all physical models, the computation procedure was carried out using Fortran.

The system of equations **(8, 13, 18 and 29)** needs to be closed by considering the following initial and boundary conditions:

$$T(x,0) = T_o$$

(32)

Each face of the parallelepipedic material is exposed to a linear plate temperature T_p (see **Fig.3**), this temperature changes with the time ranging between 7 and 39°C by using different heating/cooling rates β.

$$T(0,t)=T(L,t)=T_p=\beta t+T_o \quad \textbf{(33)}$$

where T_o is the initial temperature of the composite material.

The heat flux through the composite material can be calculated using the following formula:

$$\varphi=-k_c\left.\frac{\partial T}{\partial x}\right|_{x=0} \quad \textbf{(34)}$$

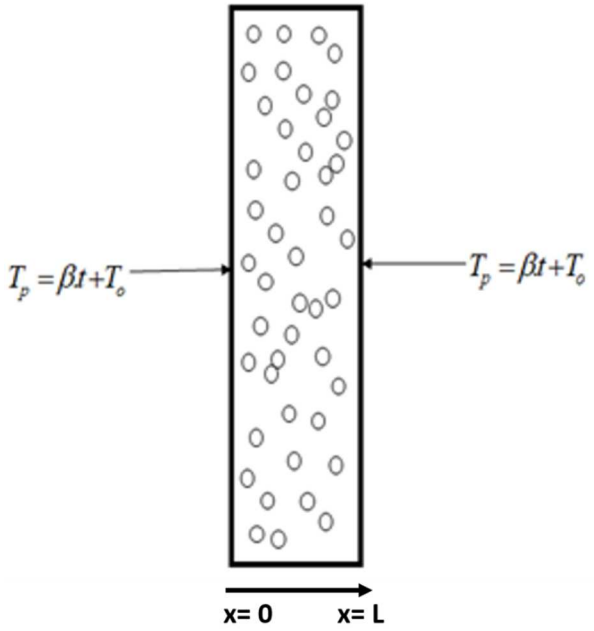

Fig.3: Boundary conditions

4. Experimental validation and parametric study

In this paragraph, we will apply physical models described in section 3, to investigate and analyze two kinds of phase transition: non-isothermal phase transition (PCM with impurities i.e. ($T_m<T_A$)) and isothermal phase transition (PCM without impurities ($T_m = T_A$)).

4.1 Non-isothermal phase transition ($T_m < T_A$)

The comparison between the experimental [32] and the numerical heat fluxes are reported in **Figs. 4-a and 4-b**. These plots illustrate the variation of the heat flux at the extremities of the composite material versus time for two heating/cooling rates ($\beta = 5.2°C/h$ and $\beta = 7.8°C/h$). The plate temperature T_p is also presented on these curves (see **Figs.4**) to indicate the variation of the recorded heat flux during the heating and cooling processes. We can remark that numerical results from different physical models are well aligned with experimental measurements. A slight difference has been noted between numerical results from the AHCM and experimental results [32]. As the calculation of the apparent heat capacity is based on the specific enthalpy function (see **Eqs. 3, 6** and **7**), the numerical results of the enthalpy method and the AHCM should be the same. However, since the enthalpy method and the AHCM method use different methods of resolution, the numerical results of these two approaches may be slightly different. Particularly during the phase transition, the computational error may be present. We can also notice that the three methods (EEM, IEM and HSM) produce practically the same numerical results. We can also mention that for the HSM, the two temperatures $T_{liquidus}$ and $T_{solidus}$ have to be judiciously chosen in order to reproduce accurately the experimental results. It is interesting to note that EEM, IEM and HSM require more calculation time than AHCM.

Whatever the heating/cooling rate, the physical models reproduce with confidence the thermal behaviour of the composite material during the phase transition process. It has been noticed that the solidification and melting processes are not symmetrical (see **Figs. 4-a and 4-b)**. In fact, during melting related to the heating rate of 7.8 °C/h (after 2 hours), the heat flux exhibits a gradual increase versus time, while during the freezing process (around 9 hours) there is a sharp variation in the heat flux. We can conclude that physical models presented in section 3 can describe correctly the phase transition within the composite material considering the asymmetric form of both enthalpy function and the apparent heat capacity for non-pure PCMs.

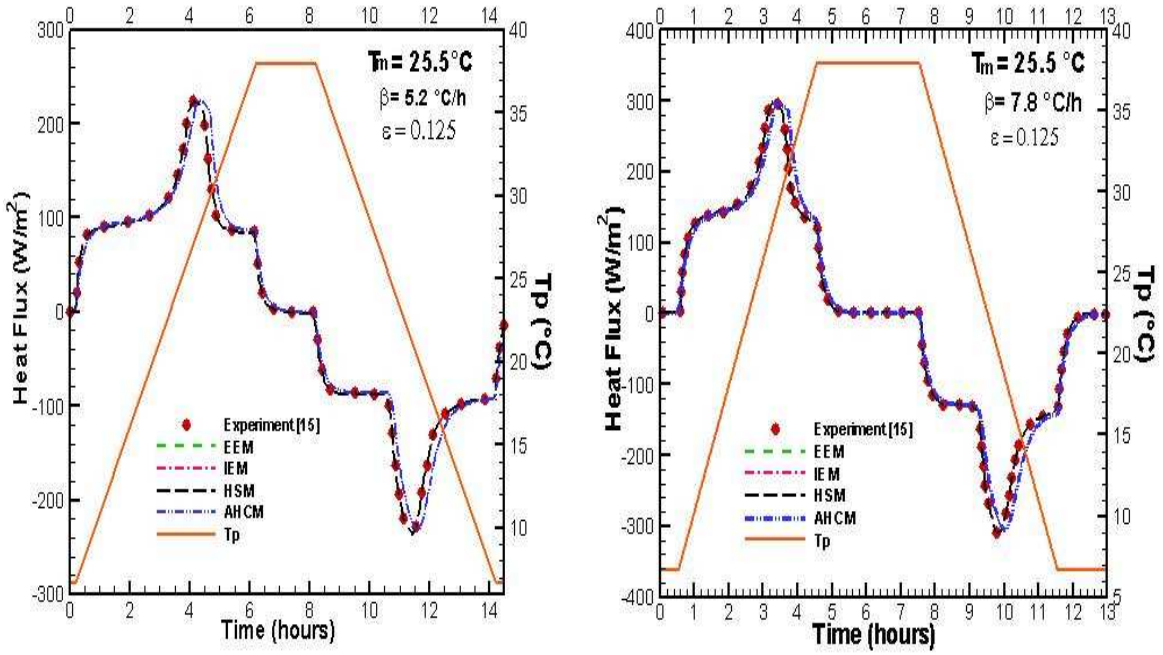

(a) **(b)**

Fig.4: Comparisons between numerical and experimental heat flux **(a)** $\beta = 5.2°C/h$ **(b)** $\beta = 7.8°C/h$

Fig.5 shows the effect of the scan rate on the numerical heat flux produced by the IEM. We note that the numerical heat flux is highly dependent on the heating/cooling rate. The phase transition time reduces as the heating/cooling rate increases. We also observe a displacement of the heat flux to the left during the cooling process and to the right during the heating process. These results can be explained by the heating/cooling rate effect on the thermal gradients inside the composite material [**18**]. For slower heating/cooling rates, the thermal gradient inside the composite material decreases but the time duration of the phase transition increases.

It is interesting to notice that the HSM permits to estimate easily the evolution of the liquid fraction (see **Eq.27**) during the phase change process (see **Fig.6**). The analysis of this figure confirms the asymmetrical nature of the melting and crystallization process due to the asymmetric form of the enthalpy function for non-pure PCMs.

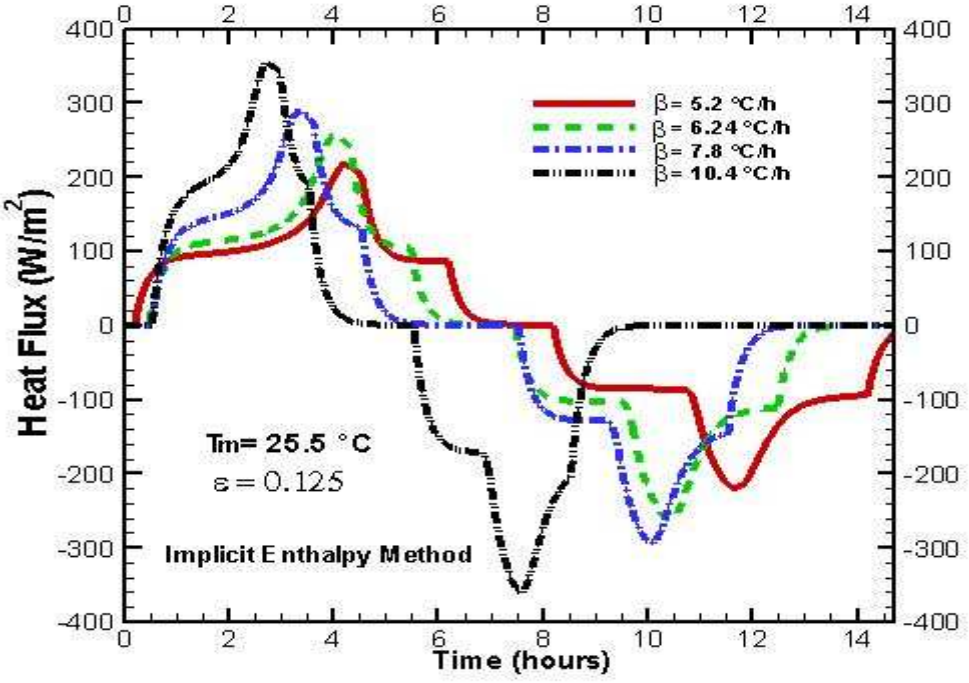

Fig.5: Numerical heat fluxes for various heating/cooling rates.

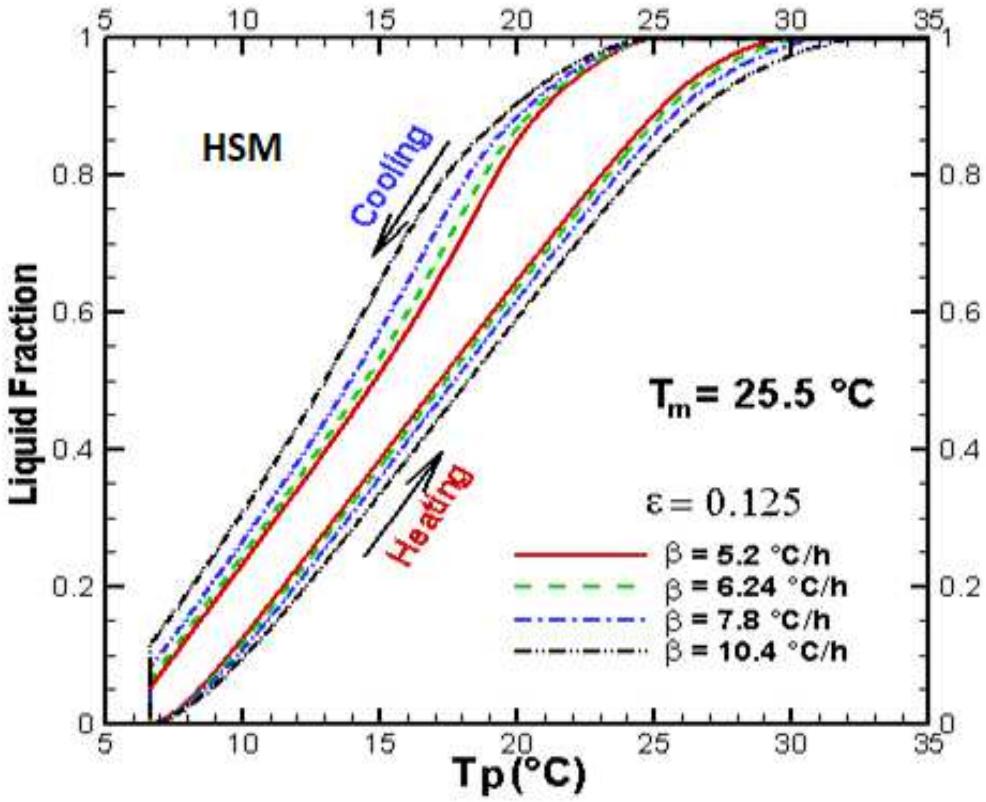

Fig.6: Numerical liquid fraction for various heating/cooling rates.

A significant hysteresis [**56-57**] in the liquid fraction is observed in **Fig.6.** To verify if the hysteresis phenomenon is present or not within the impure PCM, the temperature and the specific enthalpy at the center of the composite material during heating and cooling modes for different scan rates β are presented on **Fig.7**. The temperature is calculated using the apparent heat capacity method while the specific enthalpy is computed using the implicit enthalpy method. We remark that the temperature and the specific enthalpy function of the composite material integrating impure PCM are shifted towards the right (heating mode) and the left (cooling mode) respectively. We can note that the hysteresis phenomenon is amplified by increasing the rate of heating and cooling modes. This phenomenon is most probably due to the thermal gradients inside the composite material and to the non-symmetric enthalpy profile versus temperature.

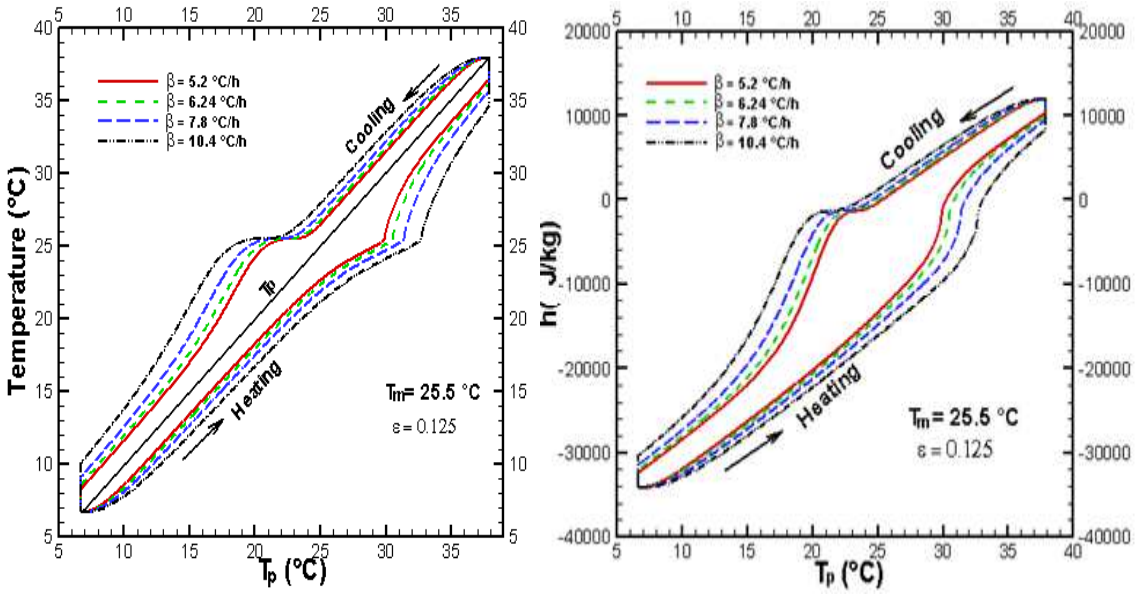

(a) **(b)**

Fig.7: Temperature **(a)** and specific enthalpy **(b)** at the center of the sample versus T_P

Fig.8 indicates the variation of numerical heat flux versus the plat temperature T_p for different values of $\mathcal{E}$. We observe that the latent energy stored or released during the phase change process in the composite material increases with increasing $\mathcal{E}$. We can also note that during the heating or cooling process, the composite material without PCM will only store/release sensible heat. This curve shows clearly the benefits of incorporating PCMs into building materials to improve their thermal inertia.

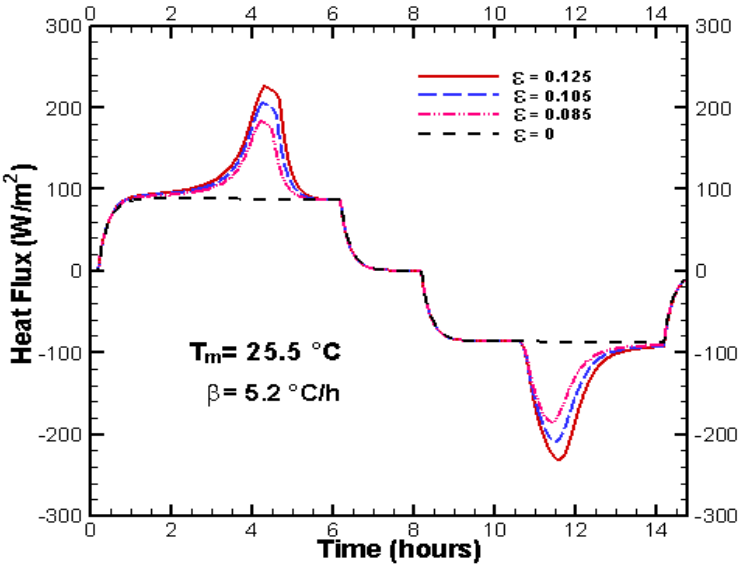

Fig.8: Numerical heat fluxes for various volume fraction of the PCM (**AHCM)**

4.2 Isothermal phase transition ($T_m = T_A$)

It is interesting to outline that both EM and AHCM encounter problems for isothermal melting (see **Eqs. (8) and (9)).** To avoid dividing by zero in **Eqs. (6) and (7),** a value of 10^{-6} is added to the denominator. Note that nodes that change phase have the impact of forcing the solution to the phase change temperature as requested. We can also note that HSM can easily address isothermal phase transition problems by using the liquid fraction function in the source term of the energy equation (see **Eq.20**).

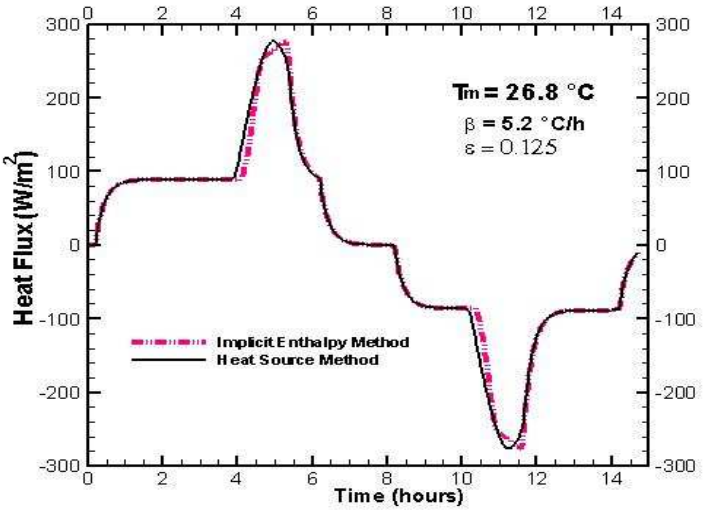

Fig.9: Comparisons between IEM and HSM (isothermal melting)

In **Fig. 9**, we have displayed the heat flux calculated by the two methods IEM and HSM when an isothermal phase transition occurs in the composite material. We notice that both methods give practically the same heat flux. There is only slight difference between the two methods in relation to the peak of the heat fluxes. The heat flux determined by HSM shows rounded peaks, while the heat flux calculated by the IEM reflects a discontinuity in enthalpy function. This discontinuity results from the numerical treatment that we used in the IEM method to avoid division by zero in equations s 6 and 7.

Figs.10-a and **10-b** display the influence of the scan rate on the numerical heat flux produced by IEM and HSM. We show that for both methods the numerical heat flux is highly dependent on the heating/cooling rate. The isothermal phase transition time decreases as the heating/cooling rate increases.

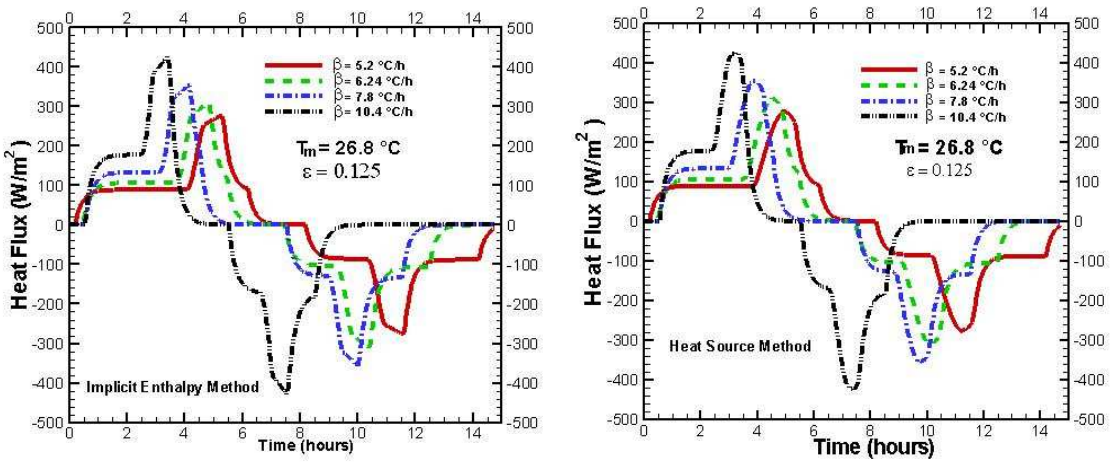

(a) **(b)**

Fig.10: Numerical heat flux for various scan rates **(a)** IEM **(b)** HSM

From the results obtained above, one can conclude that:

- Correlations between specific enthalpy and temperature as well as apparent heat capacity and temperature are highly important for EM and AHCM.
- EM, AHCM and HSM based on the assumption of the binary mixture give very satisfying results.
- The appropriate choice of liquidus and solidus temperatures allows HSM to produce similar results to those obtained with EM.

- All four models describe perfectly the asymmetrical character of melting and crystallization of impure PCM in the composite material.
- Algorithms used in EEM, IEM and HSM require more computing time than the AHCM.
- AHCM is suitable for non-isothermal melting/freezing problems if the apparent heat capacity function is available during the phase transition process.
- HSM is relevant to describe heat transfer during isothermal melting/freezing of PCM inside composite material.
- EEM, IEM and AHCM have numerical difficulties to investigate isothermal melting/freezing inside the composite material. These difficulties can be explained by the numerical discontinuity of specific enthalpy and the apparent heat capacity during solid-liquid phase change.

5. Conclusion

In this work, we presented different models such as apparent heat capacity method, enthalpy method (explicit and implicit) and heat source method for the solution of 1D heat transfer problem applied to a composite building material (mortar) dispersed with encapsulated PCM. The ability of the 1D models for analysing the thermal response of the composite binary material considered has been demonstrated by using the specific heat capacity and enthalpy functions already available in the open literature. The models have been investigated considering the phase change at a constant temperature as well occurring over a short temperature range. The effect of the heating/cooling rate and the volume fraction of the PCM on the thermal behavior of the composite material is also analyzed. A significant hysteresis phenomenon is observed during the phase transition due to the thermal gradients within the composite material as well as the non-symmetric enthalpy profile as a function of temperature.

References

[1] IEA, Energy Technology Perspectives, IEA; 2016, p. 14.

[2] A. Allouhi, Y. El Fouih, T. Kousksou, A. Jamil, Y. Zeraouli, Y. Mourad, Energy consumption and efficiency in buildings: current status and future trends. Journal of Cleaner Production 16 (2015) 118-130.

[3] L. Brady, M. Abdellatif, Assessment of energy consumption in existing buildings. Energy and Buildings 149 (2017) 142-150.

[4] S. D. Rezaei, S. Shannigrahi, S. Ramakrishna, A review of conventional, advanced, and mart glazing technologies and materials for improving indoor environment, Sol. Energy Mater. Sol. Cells 159 (2017) 26-51.

[5] M. Zinzi, S. Agnoli, Cool and green, an energy and comfort comparison between passive cooling and mitigation urban heat island techniques for residential buildings in the Mediterranean region, Energy Build. 55 (2012) 66–76.

[6] H. Omrany, A. Ghaffarianhoseini, A. Ghaffarianhoseini, K. Raahemifar, J. Tookey, Application of passive wall systems for improving the energy efficiency in buildings: A comprehensive review. Renewable and Sustainable Energy Reviews 62 (2016) 1252-1269.

[7] L. Valladares-Rendon, G. Schmid, S. Lo, Review on energy savings by solar control techniques and optimal building orientation for the strategic placement of façade shading systems, Energy Build. 140 (2017) 458–479.

[8] H. Albayyaa, D. Hagare, S. Saha, Energy conservation in residential buildings by incorporating Passive Solar and Energy Efficiency Design Strategies and higher thermal mass. Energy and Buildings, 182 (2019) 205-213

[9] V. V. Rao, R. Parameshwaran, V. V. Ram, PCM-mortar based construction materials for energy efficient buildings: A review on research trends. Energy and Buildings 158 (2018) 95-122.

[10] X. Bao , Y. Tian , L. Yuan, H. Cui, W. Tang, W.H. Fung, H. Qi, Development of high performance PCM cement composites for passive solar buildings. Energy & Buildings 194 (2019) 33–45.

[11] F. Kuznik, J. Virgone, K. Johannes. In-situ study of thermal comfort enhancement in a renovated building equipped with phase change material wallboard. Renew. Energ. 36 (2011) 1458-1462

[12] H.J. Alqallaf, E.M. Alawadhi. Concrete roof with cylindrical holes containing PCM to reduce the heat gain. Energy and Building 61 (2013) 73-80

[13] L. Royon, L. Karim, A. Bontemps. Thermal energy storage and release of a new component with PCM for integration in floors for thermal management of buildings. Energy and Buildings 63 (2013) 29-35

[14] M. Song, F. Niu, N. Mao, Y. Hu, S. Deng, Review on building energy performance improvement using phase change materials. Energy and Buildings 1581 (2018) 776-793.

[15] W. Hu, M. Song, Y. Jiang, Y. Yao, Y. Gao. A modeling study on the heat storage and release characteristics of a phase change material based double-spiral coiled heat exchanger in an air source heat pump for defrosting. Applied energy 236 (????)877-892.

[16] S. Mengjie, L. Liyuan, N. Fuxin, M. Ning, L. Shengchun, H. Yanxin. Thermal stability experimental study on three types of organic binary phase change materials applied in thermal energy storage system. Journal of Thermal Science and Engineering Applications 10 (4)

[17] Long Zhang, Jiankai Dong. Experimental study on the thermal stability of a paraffin mixture with up to 10,000 thermal cycles Thermal Science and Engineering Progress. 1 (2017) 78-87.

[18] T. El Rhafiki, T. Kousksou, A. Allouhi, W. Benomar, H. Zennouhi, A. Jamil, Y. Zeraouli, Numerical analysis of a micro-encapsulated PCM wallboard: Fluxmeter applications. Journal of Building Engineering 14 (2017) 127–133.

[19] Y. Zhang, K. Lin, Y. Jiang, G. Zhou, Thermal storage and nonlinear heat-transfer characteristics of PCM wallboard, Energy and Buildings 40 (2008) 1771-1779.

[20]J. Crank, Free and moving boundary problems. Clarendon Press (1984) Oxford.

[21]J.M. Hill, One dimensional Stefan problems : an introduction. Longman Scientific Technical (1987) Harlow.

[22] C.R. Swaminathan, V.R. Voller, Towards a general numerical scheme for solidification systems. Int. J. Heat Mass Tran. 40 (1997) 2859-68.

[23]V.Alexiades, A.D. Solomon, Mathematical modeling of melting and freezing processes. Hemisphere Publishing Corporation (1993) New York.

[24] S.Hamdaoui, M.Mahdaoui, T.Kousksou, Y.El Afou, A.Ait Msaad, A.Arid, A.Ahachad, Thermal behaviour of wallboard incorporating a binary mixture as a phase change material, Journal of Building Engineering 25 (**2019**) 120-135.

[25]T. Kousksou, A. Jamil, Y. Zeraouli, Enthalpy and apparent specific heat capacity of the binary solution during the melting process: DSC modeling, Thermochimica Acta 541 (2012) 31-41.

[26]P. W. Egolf, H. Manz, Theory and modeling of phase change materials with and without mushy regions, Int. J. Heat Mass Transfer 37 (1994) 2917-2924.

[27]M. Pomianowski, P. Heiselberg, R.L. Jensen, R. Cheng, Y. Zhang, A new experimental method to determine specific heat capacity of inhomogeneous concrete material with incorporated microencapsulated-PCM. Cem. Concr. Res. 55(2014)22-34.

[28] K. Biswas, Y. Shukla, A. Desjarlais, R. Rawal, Thermal characterization of full-scale PCM products and numerical simulations, including hysteresis, to evaluate energy impacts in an envelope application, Appl. Therm. Eng. 138 (2018) 501–512.

[29] X. Jin, H. Hu, X. Shi, X. Zhang, Energy asymmetry in melting and solidifying processes of PCM. Energy Conversion and Management 106 (2015) 608–614.

[30] Y. Zhang, Modified computational methods using effective heat capacity model for the thermal evaluation of PCM outfitted walls. International Communications in Heat and Mass Transfer 108 (2019) 104278

[31]S.N. Al-Saadi, Z.J. Zhai, Modeling phase change materials embedded in building enclosure : A review, Renew. Sustain. Energy Rev. 21 (2013) 659-673.

[32] E. Franquet, S. Gibout, P.Tittelein, L. Zalewski, J.P. Dumas, Experimental and theroretical analysis of a cement mortar containing microencapsulated PCM, Applied Thermal Engineering 73 (2014) 32-40.

[33] H. Mehling, L.F. Cabeza, Heat and Cold Storage with PCM: An up to Date Introduction into Basics and Applications, Springer, 2008.

[34] P. Lamberg, R. Lehtiniemi, Anna-Maria Henell, Numerical and experimental investigation of melting and freezing processes in phase change material storage. International Journal of Thermal Sciences 43 (2004) 277–287.

[35] I. Medved, A. Trník, L. Vozár, Modeling of heat capacity peaks and enthalpy jumps of phase-change materials used for thermal energy storage. International Journal of Heat and Mass Transfer 107 (2017) 123–132.

[36] T. Kousksou,A. Arid, A. Jamil,Y. Zeraouli, Thermal behavior of building material containing microencapsulated PCM. Thermochimica Acta 550 (2012) 42–47.

[37] Z. Younsi, H. Naji, M. Lachheb, Numerical investigation of transient thermal behavior of a wallincorporating a phase change material via a hybrid scheme. International Communications in Heat and Mass Transfer 78 (2016) 200–206.

[38]G. Zhou, Y. Yang, H. Xu, Performance of shape-stabilized phase change material wallboard with periodical outside heat flux waves. Applied Energy 88 (2011) 2113-2121.

[39] S.N. Al-Saadi, Z.J. Zhai, Modeling phase change materials embedded in building enclosure : A review, Renew. Sustain. Energy Rev. 21 (2013) 659-673.

[40] S.N. Al-Saadi, Z.J. Zhai, Systematic evaluation of mathematical methods and numerical schemes for modeling PCM-enhanced building enclosure, Energy and Building 92 (2015) 374-388.

[41] X. Jin, H. Hu, X. Shi, Xin Zhou, X. Zhang, Comparison of two numerical heat transfer models for phase change material board. Applied Thermal Engineering 128 (2018) 1331–1339

[42] A.Joulin, L. Zalewski, S. Lassue, H. Naji, Experimental investigation of thermal characteristics of a mortar with or without a micro-encapsulated phase change material, Applied Thermal Engineering 66 (2014) 171-180.

[43]F. Kuznik, K. Johannes, E. Franquet, L. Zalewski, S. Gibout, P. Tittelein, J.P. Dumas, D. David, J.P. Bédécarrats, S. Lassue, Impact of the enthalpy function on the simulation of a building with phase change material wall. Energy and Building 126 (2016) 220-229.

[44] E. Franquet, S. Gibout, J.P. Bédécarrats, D. Haillot, J.P. Dumas, Inverse method for the identification of the enthalpy of phase change materials from calorimetry experiments, Thermochimica Acta 546 (2012) 61-80.

[45] A. Frazzica, L., Recent advancements in materials and systems for thermal energy storage: An introduction to experimental characterization methods. Springer Nature Switzerland AG - 2019.

[46] C. Rathgeber, L. Miró, L. F. Cabeza, S. Hiebler, Measurement of enthalpy curves of phase change materials via DSC and T-History: When are both methods needed to estimate the behaviour of the bulk material in applications? Thermochimica Acta 596 (2014) 79-88.

[47] A. El Ouali, T. El Rhafiki, T. Kousksou, A. Allouhi, M. Mahdaoui, A. Jamil, Y. Zeraouli, Heat transfer within mortar containing micro-encapsulated PCM : Numerical approach, Construction and Building Materials 210 (2019) 422-433.

[48] Y. Zhang, X. Zhang, X. Xu, M. Lu, Derivation of thermal properties of phase change materials based on T-history method. Journal of Energy Storage 27 (2020)101062.

[49] A. Solé, L. Miró, C. Barreneche, I. Martorell, L. F. Cabeza, Review of the T-history method to determine thermophysical properties of phase change materials (PCM).Renewable and Sustainable Energy Reviews 26 (2013) 425-436.

[50] P. Tan, M. Brütting, S. Vidi, H. P. Ebert, P. Johansson, A. S. Kalagasidis, Characterizing phase change materials using the T-History method: On the factors influencing the accuracy and precision of the enthalpy-temperature curve. Thermochimica Acta 666 (2018) 212-228.

[51] M. Aadmi, M. Karkri, M. EL Hammouti, Heat transfer characteristics of thermal energy storage of a composite phase change materials: Numerical and experimental investigations, Energy 72 (2014) 381-392.

[52] A. Gounni, M. El Alami, The optimal allocation of the PCM within a composite wall for surface temperature and heat flux reduction: An experimental Approach. Applied Thermal Engineering 127 (2017) 1488-1494.

[53]M. Kheradmand, M. Azenha, J. L.B. de Aguir, J.C. Gomes, Experimental and numerical studies of hybrid PCM embedded in plastering mortar for enhanced thermal behaviour of buildings. Energy 94 (2016) 250-261.

[54] M. Iten, S. Liu, A. Shukla, Experimental validation of an air-PCM storage unit comparing the effective heat capacity and enthalpy methods through CFD simulations. Energy 155(2018)495-503.

[55]S.V. Patankar, Numerical Heat Transfer and Fluid Flow, Hemisphere Publishing Corporation, New York, 1980.

[56] L. Klimeš, P. Charvát, M. M. Joybari, M. Zálešák, F. Haghighat, K. Panchabikesan, M. El Mankibi, Y. Yuan, Computer modelling and experimental investigation of phase change hysteresis of PCMs: The state-of-the-art review. Applied Energy 263 (2020) 114572.

[57] A. Buonomano, F. Guarino, The impact of thermophysical properties and hysteresis effects on the energy performance simulation of PCM wallboards: Experimental studies, modelling, and validation. Renewable and Sustainable Energy Reviews 126 (2020) 109807.